Meteorol. Atmos. Phys. 59, 245–255 (1996)

Meteorology and Atmospheric Physics

[1] Department of Geography, University of Georgia, Athens, Georgia, U.S.A.
[2] Program in Meteorology/Climatology, Department of Geography, University of Nebraska-Lincoln, Lincoln, Nebraska, U.S.A.

A Comparison of Microwave Radiometric Data and Modeled Snowpack Conditions for Dye 2, Greenland

T. L. Mote[1] and **C. M. Rowe**[2]

With 4 Figures

Received September 23, 1994
Revised April 30, 1995

Summary

Meteorological observations were recorded at Dye 2, Greenland, during the summer of 1993 as part of a research program to identify interannual variations in melt occurrence on the Greenland ice sheet from satellite microwave data. The meteorological observations were used to drive an energy-balance model of the snowpack during 21 June to 13 July 1993. Time series of the meteorological observations and various model outputs were compared to a concurrent time series of Special Sensor Microwave/Imager (SSM/I) data for scan cells centered within 25 km of Dye 2. The satellite microwave observations clearly show an increase in snowpack emissivity at the same time that the model indicates liquid water forming in the snow. Diurnal melt-freeze cycles that occurred during mid June to early July resulted in an increase in the 37 GHz brightness temperature as great as 60 K from the dry, refrozen snow in the morning to the wet snow of some afternoons. The effects of fresh snowfall, which tend to increase the brightness temperature, and of snow growth from melt-freeze metamorphism, which tend to decrease the brightness temperature, are also apparent in the microwave observations. The results of this work demonstrate the influence of daily weather variations on the microwave emissivity in the ice sheet's percolation zone and the usefulness of swath data to diagnose the diurnal cycle of melt.

1. Introduction

Satellite-based microwave observations over the Greenland and Antarctic ice sheets have been used to determine melt occurrence, snow accumulation rates (Rotman et al., 1982; Zwally, 1977), katabatic wind intensity (Remy and Minster, 1991), and surface and depth hoar formation (Schuman et al., 1993). Such geophysical information has become increasingly important as the scientific community attempts to answer questions concerning the role of the ice sheets in various climate change scenarios. The primary concern has been the response of the mass balance of the ice sheets to potential variations in surface air temperature of the polar regions. Both surface and remotely sensed estimates of the snow accumulation and melt rates are needed to determine the impact of variations in climate on the mass balance of the ice sheets.

Recently, the melt zone of the Greenland ice sheet has been identified using radar backscatter values (Jezek et al., 1994) and radar altimeter waveforms (Ferraro, 1994). Microwave radiometric data also has been examined for indications of melt on both the Antarctic and the Greenland ice sheets on a daily, monthly and seasonal basis (Mote and Anderson, 1995; Zwally and Fiegles, 1994; Mote et al., 1993; Steffen et al., 1993). The radiometric data can be used to identify the occurrence of melt due to the increase in emissivity that results from the formation of liquid water in the snow. Liquid water in the snow also reduces the difference in brightness temperature between two channels of different frequency or polarization

from the differences associated with dry snow. However, microwave emissivity is dependent on a number of factors other than the liquid water content of the snow. Notably, the emissivity is dependent on the depth profiles of temperature, density and grain size (Zwally, 1977; Van der Veen and Jezek 1993), as well as the surface roughness (Remy and Minster, 1991) and presence of ice layers in the snowpack. As the frequency increases, a thinner layer of the snowpack is responsible for the microwave emission detected by the sensor. Therefore, daily variations in surface climate that affect the temperature, grain size, density or liquid water content of the top few centimeters of the snowpack play a large role in its microwave emissivity at high frequencies. Previous examinations of melt occurrence on the Greenland ice sheet have relied on daily averages of microwave brightness temperatures, despite the large diurnal variations that may occur in the liquid water content. This research compares swath SSM/I data to surface meteorological observations, measured snowpack temperatures, and modeled snowpack conditions for Dye 2, Greenland, from mid June to mid July 1993 to determine how variations in surface weather affect the use of satellite microwave data for melt identification.

2. The 1993 Field Season at Dye 2

The research described here was a result of one component of NASA's 1993 field season at Dye 2. Two objectives of the field program are relevant to the interpretation of melt occurrence as identified with microwave data. The first relevant objective was to collect meteorological observations during the melt season to drive an energy-balance model of the snowpack. A second objective was to collect shallow firn cores for evidence of past melt events in the snow stratigraphy and compare that record to the record of melt occurrence as interpreted from Scanning Multichannel Microwave Radiometer (SMMR) and SSM/I data. Both the model results and the core stratigraphy are being used to better understand the indications of melt identified with microwave radiometric data. The research described here is concerned with the comparison of modeled snowpack conditions to the microwave data.

Dye 2, Greenland (66 °29′ N, 46 °17′ W, 2117 m a.s.l.) lies in the percolation zone of the ice sheet,

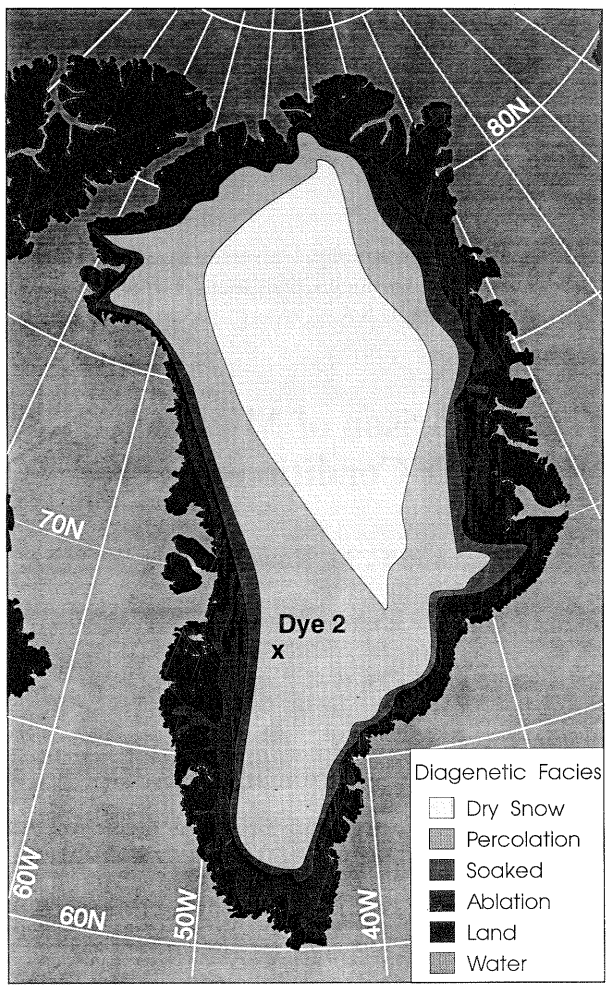

Fig. 1. Location map of Dye 2 on the Greenland ice sheet, with snow facies after Benson (1962)

a region that experiences melt but where liquid water does not completely soak the previous year's snow accumulation (Fig. 1). In the percolation zone, summer melt water percolates into the snowpack and refreezes into horizontal ice lenses and vertical ice pipes. Dye 2 is of particular interest for comparing surface conditions to microwave data because it is located in a region of the percolation zone where the microwave data indicated increasing melt frequency during the 1980s (Mote and Anderson, 1995).

Meteorological observations were taken at Dye 2 during 10 June to 13 July 1993. The measurements included hourly values of surface air temperature, snowpack temperature (at various intervals to a depth of 2 m), humidity, wind direction and speed, incoming and reflected shortwave radiation, and downwelling longwave radiation. Additional measurements of precipitation type

and amount, as well as cloud cover are available for 16 June to 13 July. These data were used to drive a one-dimensional energy and mass balance model of the snowpack that allows for melt and metamorphism of the snowpack. The model, SNTHERM.89, was developed by Rachel Jordan at the U.S. Army Cold Regions Research and Engineering Laboratory, and modified for use on the ice sheet (Jordan, 1991; Rowe et al., 1995). The model was run for the period of 21 June to 13 July and produced hourly time series that included, but were not limited to, depth profiles of temperature, liquid water content, and snow density.

3. Satellite Microwave Data

Microwave radiometric data were obtained for June and July 1993, from the SSM/I sensor aboard the Defense Meteorological Satellite Program's F-11 satellite. The satellite records radiation received at both horizontal and vertical polarizations for 19.35, 37.0, 85.5 GHz and the vertical polarization at 22.235 GHz. Because this research was an outgrowth of an examination of gridded SMMR and SSM/I data for 1979 to 1991, only channels common to both sensors were examined. The channels in common to the two sensors include both polarizations at 19.35 GHz (18 GHz for SMMR) and 37 GHz, and the vertical polarization at 22 GHz. Because the 22 GHz channel is the more sensitive to atmospheric water vapor and less sensitive to surface conditions than the other channels, it was not used in this research.

At 19.35 GHz, the footprint of the SSM/I is 69 km across track and 43 km along track, while at 37 GHz the footprint is 37 km along track and 28 km cross track (Wentz, 1991). Oversampling by the sensor allows a nominal 25 km resolution at 37 GHz. The F-11 satellite had daily overpasses of Dye 2 at approximately 0800–1000 UTC (0500 to 0700 local time) and then again around 1800–2000 UTC (1500 to 1700 local time). The passes tended to occur near the times of the lowest and highest liquid water concentrations in the snowpack so that an examination of the effect of the diurnal cycle on the snowpack's emissivity is possible.

To produce a time series of brightness temperatures for Dye 2, an inverse distance weighting approach was used for all scan cells from any one orbit that were centered within a 25 km radius of Dye 2. The number of scan cells included in the averaging for each orbit ranged from one to five with a mean of 3.6 scan cells included. The overlap in the swaths of two successive orbits often resulted in two observations during the morning or afternoon.

4. Weighted-Average Brightness Temperatures

The 37 GHz, horizontal polarization (37 H) channel was chosen for the initial comparison to modeled snowpack conditions because, for that channel, a threshold brightness temperature associated with melt has been calculated by Mote and Anderson (1995). Microwave radiometric data can be used to indicate snowpack melt due to the increase in microwave brightness temperature (at frequencies greater than 10 GHz) that occurs during melt. The emissivity of snow increases rapidly with melt due to an increase in the liquid water content of the snow. The increased emissivity is due to the high dielectric constant of liquid water, compared to that of air and ice, which strongly affects the dielectric constant of the snow-ice-air mixture. The dielectric constant is a complex number that represents a measure of the propagation characteristics of a wave through a medium (real part) and the energy losses in the medium (imaginary part). Because of the large difference in the dielectric constant of ice and water, particularly the imaginary part, a small amount of liquid water in snowpack causes a large increase in emissivity (Foster et al., 1984). In addition, the separated grains of ice that comprise a dry snowpack also cause volume scattering of the microwave radiation, an effect which is reduced by the addition of liquid water (Rango et al., 1979). The result is a strong contrast in the brightness temperature between dry snow and snow with even small amounts of liquid water. This phenomenon allows the use of a threshold brightness temperature for identifying melt occurrence. However, liquid water on the snow surface causes a decrease in emissivity due to surface reflection (Ulaby et al., 1986). No surface meltwater features were identified near Dye 2 during the summer of 1993, so the effect of surface meltwater is not a concern.

The time series of 37 H brightness temperatures was compared to SNTHERM.89 output of liquid water content averaged over the top 2 cm and the top 10 cm of the snowpack. These layers were

selected because the model results indicate that liquid water often first appears 1–3 cm below the surface of the snowpack when the air temperature is below 0 °C. This is due to radiation penetration into the snowpack and the evaporation of liquid water closer to the surface. As the model begins to indicate increased concentrations of liquid water, water becomes evident nearer to the surface and begins to percolate deeper into the snowpack. This initial formation of liquid water below the surface is also evident in liquid water content measurements at the ETH camp near the equilibrium line in West Greenland (Ohmura et al., 1991).

4.1 Snowpack Melt

The 37 H data were compared to the melt threshold value of 201.1 K for Dye 2, given by Mote and Anderson (1995). Their melt threshold values vary across the ice sheet and are partially a function of the snow accumulation rate. Regions of lower snow accumulation have lower mean annual brightness temperatures (Zwally, 1977) and lower melt threshold values. Mote and Anderson (1995) found melt threshold brightness temperatures near 230 K in the region of heavy snow accumulation on the southeast margin of the ice sheet but less than 205 K in the low accumulation region in the southwest portion of the ice sheet. Dye 2 lies in a region of relatively low accumulation and has a lower mean annual brightness temperature and melt threshold value than most locations in the melt zone of the Greenland ice sheet. The 201.1 K melt threshold value for Dye 2 seems appropriate compared to some microwave radiometric observations over a seasonal snowpack. For example, Stiles and Ulaby (1980) found 35 GHz, horizontal polarization brightness temperatures of 150–165 K for dry snow and 230–250 K for snow with 1–3 percent liquid water content. It is important to note that the 201.1 K melt threshold represents the brightness temperature for a 625 km^2 region surrounding Dye 2, in which there are almost certainly areas of both dry and wet snow during many summer days.

The afternoon observations of the 37 H brightness temperatures for each day during 9–17 June, 22–24 June and 9–12 July exceed the 201.1 K melt threshold for Dye 2. The afternoon 37 H brightness temperatures exceeded the threshold value on 1 July, by more than 35 K, and on 26 June, but only by less than 5K. The average volumetric liquid water content (m_v) in the upper 2 cm of the snowpack, as given by the SNTHERM.89 model, shows the occurrence of melt during the afternoons of 22–24 June and 10–11 July (Fig. 2). On all three days during 22–24 June, the liquid water content of the upper 2 cm of the snowpack during the time of the afternoon SSM/I overpass was greater than 6 percent; it was also greater than 6 percent on both 10 and 11 July. Although no model output are available for 9–17 June, the maximum afternoon air temperature for five of the nine days exceeded the freezing point, and the maximum afternoon temperature was within 2 K of the freezing point on the other four days. The maximum net radiation flux for those afternoons typically was greater than 150 Wm^{-2}. It is likely that melt occurred in the upper few centimeters with adequate net radiation even though surface air temperatures were slightly below the freezing point. Even if melt did not occur at Dye 2 on some of those days, it is quite likely that melt did occur at lower elevations that were within some of the scan cells included in the average. The surface air temperatures were also at or above freezing on the afternoons of 22–24 June and 10–13 July.

Melt was also indicated in the upper 2 cm of the modeled snowpack before the afternoon SSM/I overpass on 28 June as the surface air temperature rose above freezing, but the model output indicates that the surface had refrozen by the time of the sensor overpass. The 37H brightness temperature during the afternoon overpass of 28 June (188.3 K) is less than the threshold value (201.1 K), giving no indication of melt (Fig. 2). The model provides no indication of melt in the top 2 cm of the snowpack during the afternoon of 1 July, and the surface air temperature was 5 K lower than the freezing point at the time of the SSM/I overpass. However, the 37H brightness temperatures during the afternoon overpasses were 236.2 K at 18 UTC (1500 local time) and 213 K at 20 UTC (1700 local time), which are both above the melt threshold value (Fig. 2). Although no melt was indicated in the top 2 cm, there was an indication of melt in the top 10 cm. Despite the low surface air temperatures, enough net radiation (150–200 Wm^{-2}) was available to cause the model to simulate melting. The low density of the fresh snow that fell during the morning of 1 July likely allowed pene-

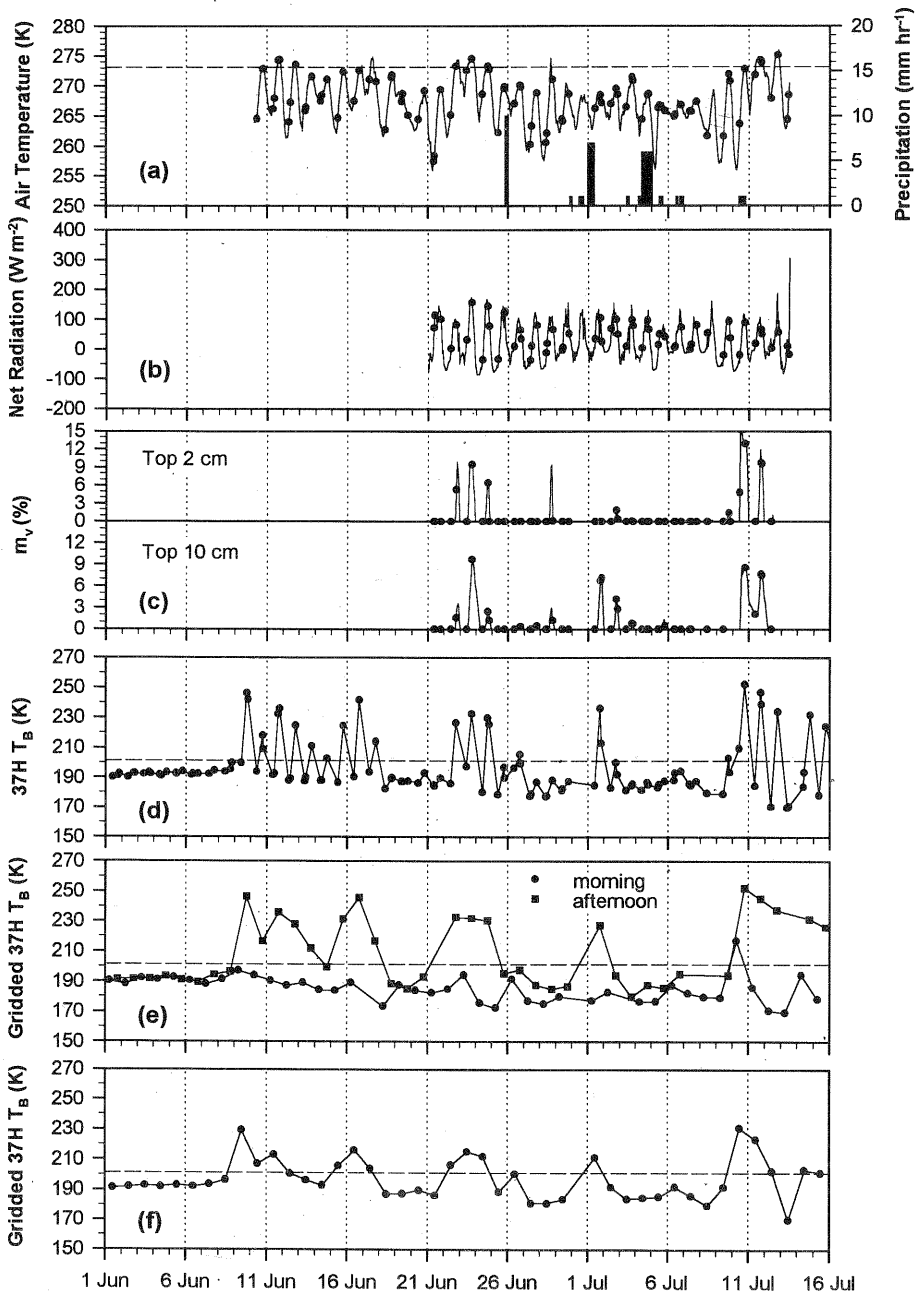

Fig. 2. Meteorological data, modeled snowpack conditions and concurrent SSM/I brightness temperature time series for June and July 1993 at Dye 2, Greenland. Surface air temperatures (solid line), surface air temperatures taken at the time of SSM/I overpasses (circles), and precipitation (bars) (a); modeled net radiation (solid line), and modeled net radiation at the time of an SSM/I overpass (circles) (b); modeled liquid water content averaged in the top 2 and top 10 cm of the snowpack (solid line), and modeled liquid water content at the time of an SSM/I overpass (circles) (c); weighted average 37H brightness temperatures (d); morning (circles) and afternoon (squares) gridded 37H brightness temperatures (e); daily averaged, gridded 37H brightness temperatures (f)

tration of radiation further into the snowpack, producing melt below but not within the top 2 cm of the snowpack. It is also likely that the fine-grained fresh snowfall reduced the scattering of microwave radiation and contributed to the increased brightness temperatures on the afternoon of 1 July.

In one case, the model output indicated liquid water in the snowpack, but the 37H brightness temperatures were not elevated. The 11 July m_v for the top 10 cm of the snow showed approximately 3 percent liquid water content, although the model output showed the top 2 cm as dry. Although the model indicates some liquid water in the top 10 cm, the 37 H brightness temperature for the 11 July morning overpass was only 184.3 K. This is in contrast to the observations and model output during the afternoon of 1 July, in which the model output shows liquid water in the snowpack below a dry layer, but the microwave data show a relatively high brightness temperature (236.2 K at 18 UTC). This difference at

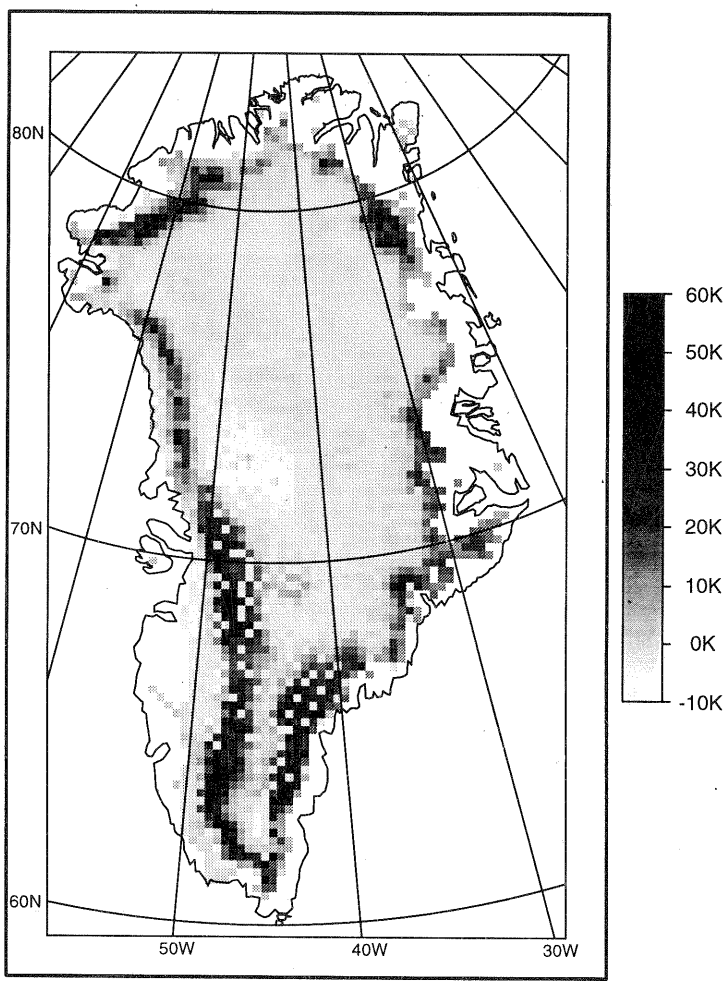

Fig. 3. Afternoon 37H brightness temperatures minus morning 37H brightness temperatures for 23 June 1993 across the Greenland ice sheet

first suggests that the model may not be adequately handling the percolation and refreezing of melt water in the snowpack, and the top 10 cm of the snowpack was actually dry on 11 July. However, the difference between the afternoon of 1 July and the morning of 11 July was that on 11 July the top 2 cm was a refrozen snow layer while on 1 July the surface of the snowpack was freshly fallen snow. The large-grained, refrozen upper layers on the morning of 11 July would have scattered the radiation emitted from the underlying wet layers, reducing the brightness temperature, while the fine-grained fresh snow on 1 July did not.

Because all days in which melt occurred showed evidence of refreezing during the morning, the afternoon-morning brightness temperature difference was examined for all available SSM/I data over the Greenland ice sheet. The daily maps of the gridded brightness temperatures for the afternoon minus the morning observations were examined for the period of 1 June to 19 July 1993. As an example, a map of the afternoon minus the morning brightness temperatures for 23 June, a day with afternoon melt at Dye 2, shows differences as great as 60K in some locations in the south and southwest margins of the ice sheet (Fig. 3). A region of brightness temperature differences greater than 30 K follows the margin of the south dome of the ice sheet from approximately 65° N on the eastern margin to approximately 68° N on the western margin of the south dome. This area of large brightness temperature differences extends from the margin of the ice sheet to approximately 1800 m a.s.l. The large diurnal variation in brightness temperature associated with afternoon melt and morning refreeze that was identified at Dye 2 is also evident across most of the ice sheet that is known to experience melt.

4.2 Precipitation and Metamorphism

Only the afternoon of 26 June had a brightness temperature above the threshold value but was

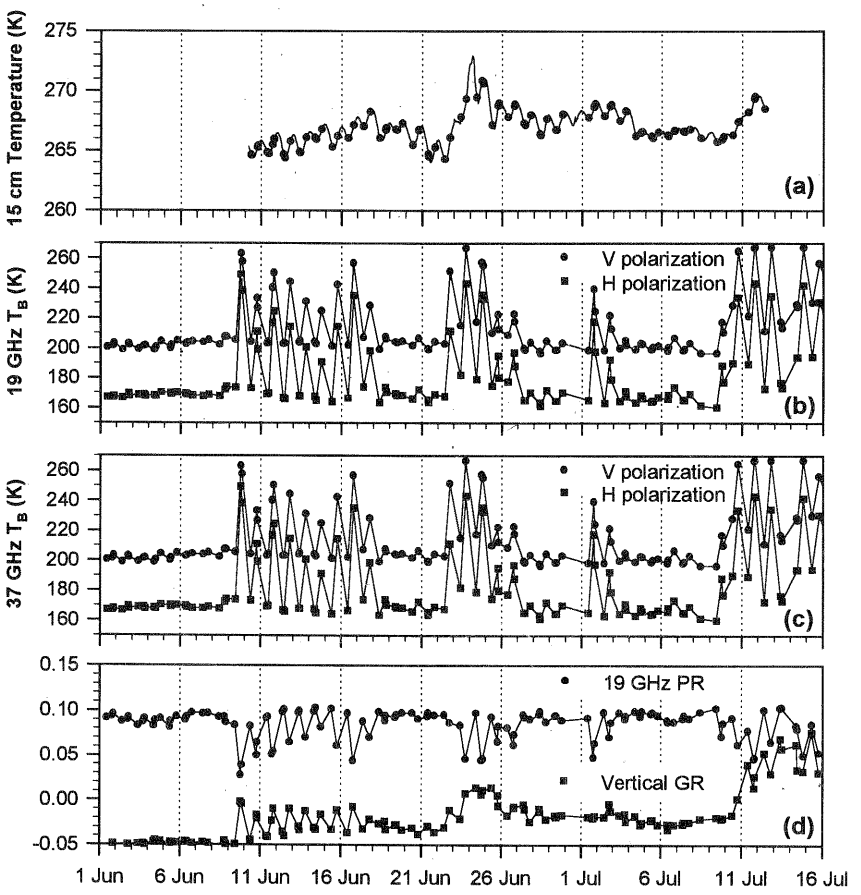

Fig. 4. Measured snowpack temperatures and normalized differences of the SSM/I brightness temperatures during June and July 1993 for Dye 2, Greenland. Measured snowpack temperatures at a depth of 15 cm (solid line), and measured snowpack temperatures at times of SSM/I overpasses (circles) (a); 19 GHz vertical (circles) and horizontal (squares) brightness temperatures (b); 37 GHz vertical (circles) and horizontal (squares) brightness temperatures (c); 19 GHz polarization ratio (circles) and vertical gradient ratios (squares) (d)

not associated with some clear indication of melt in the model output. The morning of 26 June also had a brightness temperature approximately 10 K greater than morning brightness temperatures for days immediately before and after that day. An initial hypothesis was that the increase in brightness temperature was due to warming of the snowpack. The snowpack temperature measured at 15 cm was 272 K at 3 UTC on 24 June (Fig. 4) and the temperature measured at 20 cm was 270 K at 18 UTC on 24 June. In both cases, the temperature were higher than at any other time from 11 June to 13 July at the respective depths in the snowpack. The warming of the snow apparently was due to heat transported into the snowpack by the meltwater formed on 22–24 July and the latent heat released during the refreezing of the meltwater. However, the 15 cm snowpack temperatures were between 266 and 268 K during both 26 and 27 June, while the 37H brightness temperature decreased from 205.4 K on the afternoon of 26 June to 177.5 K on the morning of 27 June. Because of the linear relationship between physical temperature and brightness temperature, the variations in physical temperature cannot explain the higher than expected 37H brightness temperatures on 26 June.

Another possible explanation of the higher than expected brightness temperatures was the location of the scan cells included in the weighted average. On the afternoon of 26 June, the scan cell with the highest 37H brightness temperature (216.0 K), was centered 24.1 km to the west- northwest of Dye 2. By plotting the location of the scan cell on a topographic map of Greenland, one can see that the footprint of the scan cell included a region as much as 200 m lower than Dye 2. It is possible that the snowpack at lower elevations within that scan cell was experiencing some melt, raising the brightness temperature recorded for that scan cell.

Although the location of the individual scan cells may explain the higher than expected afternoon 37H brightness temperature on 26 June, the

morning brightness temperature that day was also approximately 10 K higher than other mornings in late June. This is likely due to the 5 cm of fresh snow that fell on the evening of 25 June (Fig. 2). The fine-grained snow that fell may have reduced the microwave scattering, resulting in the increased brightness temperature. This may also explain why the brightness temperatures on 5 July are approximately 5 K higher than on other days without melt in early July. Dye 2 had approximately 12 cm of fresh snow during 3–6 July, mostly on 4 July. The snowfall that occurred on 30 June and 1 July does not show the same effect in the morning 37 H brightness temperatures, but melt occurred immediately after the snowfall ended. The melt likely resulted in immediate metamorphism of the fresh snow, which increased the snow grain size and eliminated any increase in emissivity due to the fresh snow.

Melt-freeze metamorphism results in increased grain size, which increases the effect of volume scattering and reduces the brightness temperatures. At Dye 2, a result of this process is the downward trend in morning brightness temperatures from approximately 190 K during early June to 170 K in mid July. These changes appear in steps that correspond to the various melt periods. The morning brightness temperatures decreased from slightly greater than 190 K during the first week of June to approximately 185 K after the 9–17 June melt period. After the 22–24 June melt period, the morning brightness temperatures decreased to approximately 180 K, and then decreased to about 170 K during the melt period that began 9 July.

4.3 Normalized Differences of Brightness Temperatures

While our research has used a single-channel threshold method to identify melt events, Steffen et al. (1993) used multi-channel, normalized difference measure of the 19 and 37 GHz brightness temperatures for melt identification. Individually, the time series for each of the four SSM/I channels had similar characteristics during June and July 1993 at Dye 2. To determine how the evolution of the snowpack affected the other SSM/I channels, normalized differences of brightness temperatures for channels of different frequencies or polarizations were calculated.

The polarization ratio (PR) at a frequency f is defined as:

$$PR_f = (T_{B,v} - T_{B,h})/(T_{B,v} + T_{B,h}) \quad (1)$$

where $T_{B,v}$ is the vertical polarization brightness temperature at that frequency and $T_{B,h}$ is the horizontal polarization brightness temperature.

The gradient ratio (GR) at a polarization p is defined as:

$$GR_p = (T_{B,37} - T_{B,19})/(T_{B,37} + T_{B,19}) \quad (2)$$

where $T_{B,19}$ is the 19 GHz brightness temperature for that polarization and $T_{B,37}$ is the 37 GHz brightness temperature. In particular, the GR was examined for the effect of meltwater penetration on the emissivity at different frequencies. Due to the longer wavelength of radiation, the 19 GHz channels are sensitive to radiation emitted from a greater depth into the snowpack than are the 37 GHz channels. Thus, the GR tends toward zero or become positive during melt episodes.

The 19V, 19H and 37V channels show the same indications of melt as the 37H channel. Additionally, both of the normalized differences of the channels, the PR and GR, show evidence of the effects of snowpack melting. During the daily melt-refreeze cycles of 9–17 June, the PR and GR both tended toward zero during afternoon melting (Fig. 4). Throughout the study period, the PR values tended toward zero during the same afternoons that had increased brightness temperatures for the 37H channel.

During the melt period of 22–24 June, both the morning and afternoon GR values tended toward zero. Although GR values near zero are sometimes associated with the occurrence of melt (Steffen et al., 1993), there was no evidence from the meteorological data, model output or the use of a single-channel threshold to support the conclusion that melt occurred during the morning SSM/I overpass. The GR values on the mornings of 22–24 June may have been due to the warming of the underlying snowpack that is evident in the temperature profile of the snowpack during this period. The colder, refrozen snow near the surface resulted in a lower brightness temperature at 37 GHz than at 19 GHz, which is apparent in the GR for 24 and 25 June.

A step-change in the GR values from predominately negative to predominately positive values occurred on 10–11 July. This coincides with a

period when the model showed significant melt and liquid water percolation to 15–20 cm. The meltwater percolation occurred during the afternoon of 10 July and the subsequent warming of the snowpack with meltwater refreezing occurred late on 10 July and into the morning of 11 July (Fig. 4). The increased physical temperature of the snowpack at 15–20 cm as well as the increase in emissivity due to the introduction of liquid water at that depth may be the reason for increased brightness temperatures at 19 GHz and a positive GR. In general, both the PR and GR time series can be used to identify the melt periods that are also evident in the time series of the 37H brightness temperatures.

5. Gridded Brightness Temperatures

The field work conducted at Dye 2 was an outgrowth of research that has used gridded SMMR and SSM/I brightness temperatures available from the National Snow and Ice Data Center (NSIDC) for identifying melt occurrence on the Greenland ice sheet. In the NSIDC data set, all scan cells that were centered within a given grid cell were averaged for each day (beginning at 0 UTC). This approach results in the loss of diurnal variations in brightness temperatures. One objective of the present work was to compare both the swath data and gridded data for Dye 2 to the surface meteorological data and snowpack conditions to determine what information is lost in the daily averaging procedure.

The swath brightness temperatures were binned into the polar stereographic grid defined by NSIDC using three different averaging periods. First, observations were averaged into either morning or afternoon grids; then, all observations were averaged on a daily basis. In all three cases, no weighting was applied to produce the averages. If the center of a scan cell was within the square 25×25 km grid cell that contains Dye 2, it was included in the average. Thus, the spatial resolution of the three binned time series is comparable to that of the weighted average time series.

Both the twice-daily and daily time series seem to preserve the dominant features of the time series from the weighted average of the orbital data. The daily gridded and the afternoon gridded data indicated that surface melt was occurring on 9–11, 15–17 and 22–24 June, 1 July and 10–12 July (Fig. 2). However, the time series from the daily averaged data did not exceed the threshold value associated with melt on 12–14 June, while the time series from the gridded data of afternoon overpasses did not indicate melt on 14 June. The brightness temperatures in the weighted average time series did indicate melt each afternoon during 9–17 June, although the 37H brightness temperature exceeded the melt threshold by less than 2K on the afternoon of 14 June. Because no model output is available before 16 June, it is uncertain whether any melt actually occurred on the afternoon of 14 June. The surface temperatures and net radiation flux for that afternoon indicate that conditions were conducive to modest, radiation-induced melting. Additionally, only a small increase in the threshold value associated with melt could result in the conclusion that no melt occurred that afternoon with any of the three time series presented here.

One problem with the daily gridded data is the occurrence of two overpasses in either the morning or in the afternoon that are subsequently included in the averaging. The result is a possible bias toward the morning or afternoon values in the daily average. For example, two overpasses of the sensor occurred on the afternoon of 11 July, while only one morning overpass occurred. Additionally, the morning overpass only had three scan cells included in the average, while the two afternoon overpasses had five scan cells on the 18 UTC overpass and four cells on the 19 UTC overpass included in the average. As a result, the daily average is heavily weighted toward the afternoon conditions. The weighted average of scan cells for the 37H channel during the 9 UTC overpass showed a brightness temperature of 184.3K, while the afternoon overpasses at 18 and 19 UTC showed 37H brightness temperatures of 246.7 K and 238.9 K, respectively. The daily average for the gridded data showed a brightness temperature of 224 K for the grid cell that includes Dye 2. However, averaging the scan cells from the two afternoon overpasses and then averaging that result with the average of the scan cells from the morning overpass yields a daily average of only 214 K.

The process of binning data into a grid, compared to the inverse-distance weighted average was also examined. This was done by comparing the morning and afternoon gridded data to the

orbital data for dates on which there was only one morning or afternoon overpass of the sensor. The brightness temperatures produced by the binning or weighted average processes were nearly identical and would not affect the identification of melt. One exception was the afternoon of 14 June, when the afternoon gridded brightness was approximately 1 K less than the melt threshold and the inverse-distance weighted average produced a brightness temperature about 1 K above the melt threshold.

6. Conclusions

Meteorological observations recorded at Dye 2, Greenland, during June and July 1993 were used to drive an energy-balance model of the snowpack. The liquid water content values output from the model and the various meteorological observations were compared to time series of Special Sensor Microwave/Imager (SSM/I) data averaged for scan cells centered within 25 km of Dye 2.

Diurnal melt-freeze cycles that occurred during mid June to early July are evident both by an increase and subsequent decrease in the microwave brightness temperatures and from the formation of liquid water as shown in the model output. Additionally, the effects of the melt-freeze metamorphosis of the snow and new snow accumulation are evident in the brightness temperature time series. These time series demonstrate that a brightness temperature threshold for a single channel of microwave data can be used for melt identification, particularly if other geophysical characteristics of the snowpack are also considered. One improvement on the single-channel threshold approach might be the addition of an afternoon-morning difference for a given channel. A threshold of the afternoon- morning brightness temperature difference could be used in conjunction with a single-channel threshold to account for melt occurring throughout the low-sun hours, which would not be detected by using an afternoon-morning difference alone.

Due to the relatively coarse resolution of passive microwave data, heterogeneous snow conditions within a grid cell or scan cell introduce difficulty in interpreting the microwave data. This is particularly true when comparing surface conditions at one point to scan cells that may include information from sites nearly 50 km away from the location of interest. The use of modeled surface conditions for comparison to the microwave data partially alleviates this problem because the modeled snowpack conditions are probably more representative of mixed conditions than a firn core or snow pit.

The different approaches to spatial and temporal averaging of the microwave data also introduce uncertainties into interpreting the resultant time series. To illustrate these problems, the time series produced from an inverse-distance weighted average of scan cells within 25 km of Dye 2 was compared to data binned into a 25 × 25 km grid cell that includes Dye 2, averaged on either a daily or twice-daily basis. The gridding process used can make a substantial difference in the estimated brightness temperature for a given location, particularly if the scan cells included in a daily average tend to be clustered more in the morning or afternoon.

Acknowledgments

This work was supported by the Polar Oceans and Ice Sheets Program of the National Aeronautics and Space Administration, grant NAGW-1266, and by the NASA Global Change Fellowship Program, training grant NGT-30127, both to the University of Nebraska-Lincoln. The authors thank M. R. Anderson, E. J. Ferraro, K. C. Jezek, K. C. Kuivinen, and I. H. H. Zabel for assistance in collecting observations at Dye 2.

References

Benson, C. S., 1962: Stratigraphic studies in the snow and firn of the Greenland ice sheet, CRREL Res. Rep. 70. CRREL, Hanover, NH, 93 pp.

Ferraro, E. J., 1994: Analysis of Airborne Radar Altimetry Measurements of the Greenland Ice Sheet. Ph.D. Dissertation, University of Massachusetts, Amherst, MA, 164 pp.

Foster, J. L., Hall, D. K., Chang, A. T. C., Rango, A., 1984: An overview of passive microwave snow research and results. *Rev. Geophys. Space Res.*, **22**, 195–208.

Jezek, K. C., Gogineni, P., Shanableh, M., 1994: Radar measurements of melt zones on the Greenland ice sheet. *Geophys. Res. Letters*, **21**, 33–36.

Jordan, R., 1991: A one-dimensional model for a snow cover: technical documentation for SNTHERM.89 Special Report 91–16, U.S. Army Crops of Engineers, Cold Regions Research and Engineering Laboratory, Hanover, NH.

Mote, T. L., Anderson, M. R., Kuivinen, K. C., Rowe, C. M., 1993: Passive microwave-derived spatial and temporal variations of summer melt on the Greenland ice sheet. *Ann. Glaciol.*, **17**, 233–238.

Mote, T. L., Anderson, M. R., 1995: Variations in snowpack melt on the Greenland ice sheet based on passive microwave measurements. *J. Glaciol.*, **17**, 51–60.

Ohmura, A., Steffen, K., Blatter, H., Greuell, W., Rotach, M., Konzelmann, T., Laternser, M., Ouchi, A., Steiger, D., 1991: Energy and Mass Balance During the Melt Season at the Equilibrium Line Altitude, Paakitsoq, Greenland Ice Sheet: Progress Report No. 1. Department of Geography, Swiss Federal Institute of Technology, Zurich, 118 pp.

Rango, A., Chang, A. T. C., Foster, J. L., 1979: The utilization of spaceborne microwave radiometers for monitoring snowpack properties. *Nord. Hydrol.*, **10**, 25–40.

Remy, F., Minster, J. F., 1991: A comparison between active and passive microwave measurements of the Antarctic ice sheet and their association with the surface katabatic winds. *J. Glaciol.*, **37**, 3–10.

Rotman, S. R., Fisher, A. D., Staelin, D. H., 1982: Inversion for physical characteristics of snow using passive radiometric observations. *J. Glaciol.*, **28**, 179–185.

Rowe, C. M., Kuivinen, K. C., Jordan, R., 1995: Simulation of summer snowmelt on the Greenland ice sheet using a one-dimensional model. *J. Geophys. Res.*, **100**, 16,265–16,273.

Schuman, C. A., Alley, R. B., Anandakrishnan, S., 1993: Characterization of a hoar-development episode using SSM/I brightness temperatures in the vicinity of the GISP-2 site, Greenland. *Ann. Glaciol.*, **17**, 183–188.

Steffen, K., Abdalati, W., Stroeve, J., 1993: Climate sensitivity studies of the Greenland ice sheet using satellite AVHRR, SMMR, SSM/I and in situ data. *Meteorol. Atmos. Phys.*, **51**, 239–258.

Stiles, W. H., Ulaby, F. T., 1980: The active and passive microwave response to snow parameters: 1. Wetness. *J. Geophys. Res.*, **85**, 1037–1044.

Ulaby, F. T., Moore, R. K., Fung, A. K., 1986: *Microwave Remote Sensing, Active and Passive*, vol. 3. Reading, MA: Addison-Wesley, 2162 pp.

van der Veen, C. J., Jezek, K., 1993: Seasonal variations in brightness temperature for central Antarctica. *Ann. Glaciol.*, **17**, 300–306.

Wentz, F. J., 1991: SSM/I Antenna Temperature Tapes User's Manual, Revision 1. Remote Sensing Systems, Santa Rosa, CA, 70 pp.

Zwally, H. J., 1977: Microwave emissivity and accumulation rate of polar firn. *J. Glaciol.*, **18**, 195–215.

Zwally, H. J., Fiegles, S., 1994: Extent and duration of Antarctic surface melt. *J. Glaciol.*, **40**, 463–476.

Authors' addresses: Thomas L. Mote, Department of Geography, University of Georgia, 204 GGS Building, Athens, GA 30602-2502, U.S.A.; C. M. Rowe, Program in Meteorology/Climatology, Department of Geography, University of Nebraska-Lincoln, Nebraska, U.S.A.